NANO LETTERS

LETTER

pubs.acs.org/NanoLett

Optical Impedance Matching Using Coupled Plasmonic Nanoparticle Arrays

P. Spinelli,*[,†] M. Hebbink,[†] R. de Waele,[†] L. Black,[‡] F. Lenzmann,[‡] and A. Polman[†]

[†]Center for Nanophotonics, FOM-Institute AMOLF, Science Park 104, 1098 XG Amsterdam, The Netherlands

[‡]Energy Research Center of The Netherlands ECN, P.O. Box 1, 1755 ZG Petten, The Netherlands

ABSTRACT: Silver nanoparticle arrays placed on top of a high-refractive index substrate enhance the coupling of light into the substrate over a broad spectral range. We perform a systematic numerical and experimental study of the light incoupling by arrays of Ag nanoparticle arrays in order to achieve the best impedance matching between light propagating in air and in the substrate. We identify the parameters that determine the incoupling efficiency, including the effect of Fano resonances in the scattering, interparticle coupling, as well as reso nance shifts due to variations in the near-field coupling to the substrate and spacer layer. The optimal configuration studied is a square array of 200 nm wide, 125 nm high spheroidal Ag particles, at a pitch of 450 nm on a 50 nm thick Si_3N_4 spacer layer on a Si substrate. When integrated over the AM1.5 solar spectral range from 300 to 1100 nm, this particle array shows 50% enhanced incoupling compared to a bare Si wafer, 8% higher than a standard interference antireflection coating. Experimental data show that the enhancement occurs mostly in the spectral range near the Si band gap. This study opens new perspectives for antireflection coating applications in optical devices and for light management in Si solar cells.

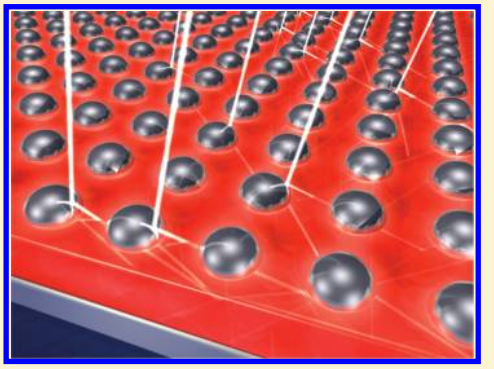

KEYWORDS: Metal nanoparticles, plasmonics, antireflection coatings, light coupling, scattering

The coupling of light into a dielectric material is always associated with (usually unwanted) reflection. Reflection can be reduced by using a dielectric interference coating. These coatings are optimized for a given wavelength and incident angle and thus reduce reflectance over a relatively narrow bandwidth. Recently, metal nanoparticles deposited onto a substrate have been studied to increase the coupling of light into a substrate.[1,2] These particles interact strongly with the incident light and preferentially scatter light into the high-index substrate, leading to enhanced transmittance and thus reduced reflectance. The resonant scattering is due to plasmon resonances in the metallic particles and leads to reduced reflection over a broad spectral range.

So far, most experimental work on antireflection (AR) effects from particle scattering has focused on ensembles of metal nanoparticles made using self-assembly, which leads to random nanoparticle configurations, with limited control over the particle geometry.[3−9] As a result, the effect of particle geometry has not been systematically studied experimentally. Theoretical work, using finite-difference time domain (FDTD) simulations, has focused mostly on the scattering from single particles, thereby neglecting interparticle coupling.[10−12] Thus, so far no systematic studies have been made of the critical parameters that determine the optimum impedance matching of light using metal nanoparticle arrays. Moreover, no previous work has made a systematic comparison between particle arrays and standard dielectric AR coatings.

In this paper, we perform a systematic study of the coupling of light into a crystalline silicon substrate, through scattering of light from silver nanoparticle array geometries. We investigate the effect of particle shape, size, and array pitch on the incoupling, using both experiment and simulation. Furthermore, we study the effect of a dielectric spacer layer between the particle array and the substrate. We find that an optimized array of Ag nanoparticles, combined with a Si_3N_4 spacer layer of suitable thickness, yields better light incoupling into a silicon substrate over a broad spectral range than a traditional Si_3N_4 interference AR coating.

We identify the parameters that determine the incoupling efficiency, including the effect of Fano resonances in the scattering, interparticle coupling, as well as resonance shifts due to variations in the near-field coupling to the substrate and the dielectric spacer layer. The insights given in this paper provide general guidelines for the optimization of impedance matching using plasmonic scattering, opening new perspectives for application of these coatings in photovoltaics,[13,14] photodetectors, and optical components in general. For the photovoltaic application, the use of metal nanoparticles as AR coating provides additional benefits, such as an enhanced optical path length as a result of angular redistribution of light inside the semiconductor and light trapping in thin-film solar cells by coupling to waveguide modes.[15]

Light Scattering from Single Particles: FDTD Simulation. As a first step, we use three-dimensional FDTD simulations[16] to study the basic case of a single silver nanoparticle on top of a

Received: January 27, 2011
Revised: March 7, 2011
Published: March 16, 2011

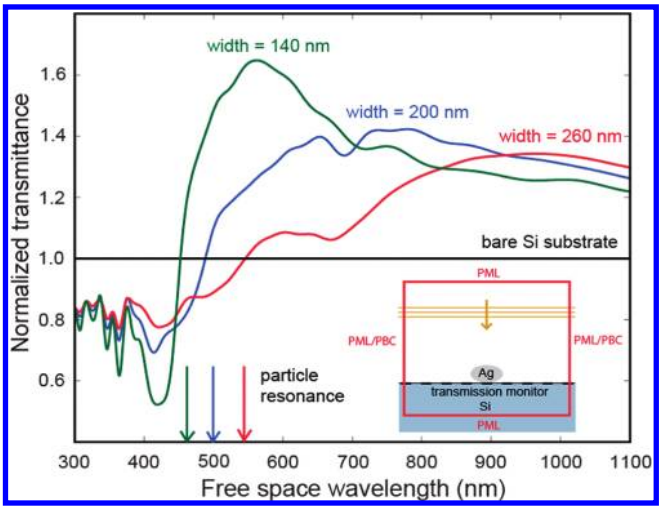

Figure 1. Transmittance spectrum for three different single Ag spheroids with 175 nm height and 140 nm (green), 200 nm (blue), and 260 nm (red) width, on top of a Si substrate, calculated using FDTD. Data are normalized to the transmittance for a bare Si substrate. For each particle, the transmission is enhanced for wavelengths above the Ag particle plasmon resonance and suppressed for wavelengths below (Fano effect). The inset shows a schematic of the simulation geometry.

semi-infinite silicon substrate. The FDTD simulation geometry is shown schematically in the inset of Figure 1. A broad-band pulse (wavelength 300−1100 nm) is used to simulate a plane wave incident on the particle from the top. A monitor positioned at the surface measures the total power that is coupled into the Si substrate (transmittance). Perfectly matched layer (PML) boundary conditions were used in the incident direction to prevent nonphysical scattering at the boundaries, thereby effectively simulating an infinitely thick Si layer. PMLs are also used at the boundaries of the simulation volume, to simulate a single-particle configuration. Optical constants for Ag were taken from Palik[17] and fitted using a combined Drude, Lorentz, and Debye model; data for Si were taken from Palik as well.

Figure 1 shows the transmission spectrum of three different single Ag spheroids on top of a Si substrate, normalized to the transmission spectrum of a bare Si substrate. Particle height is 175 nm, and particle widths are 140 nm (green), 200 nm (blue), and 260 nm (red), respectively. The arrows in the graph indicate the plasmon resonance wavelengths for each of the particles derived from the peak in the simulated scattering spectrum. Note that the values of the normalized transmittance depend on the size of the simulation box ($1 \times 1\ \mu$m); the data in Figure 1 therefore only serve to study the spectral trends in the transmission. Absolute values will be addressed in the next section when studying particle arrays.

For wavelengths above resonance, the transmission is enhanced by the presence of the nanoparticle. The mechanism behind this effect is the scattering of light by the dipolar resonance of the particle, which redirects the light preferentially into the high-index substrate.[10,18] On the other hand, a reduced transmission is consistently observed below the particle resonance for each of the three particle sizes. This reduction occurs due to a Fano effect, i.e., the destructive interference between scattered and unscattered light that occurs below resonance.[19−22] Figure 1 therefore shows that proper tuning of the plasmonic resonance wavelength is important in order to optimize the light coupling into the substrate.[10−12]

Light Scattering from Particle Arrays: FDTD Simulation. Next, we studied the case of a square array of Ag nanoparticles on top of a Si substrate. The FDTD geometry is identical to the single-particle case (inset in Figure 1), with the exception of the use of periodic boundary conditions (PBCs) in the lateral direction instead of PML boundary conditions. The array pitch is thus equal to the simulation box size.

We have simulated the transmission spectrum for different Ag spheroid array geometries on Si. For each configuration, we determine an incoupling enhancement factor by integrating the enhancement over the spectrum and weighting to the AM1.5 standard solar spectrum in the 300−1100 nm spectral range. Figure 2 shows the enhancement factor for geometries with varying particle width (a), particle height (b), and array pitch (c). On the right axis, the absolute transmittance is shown for reference. The enhancement factor is taken relative to that for a bare Si layer. The enhancement for a Si wafer coated with an 80 nm thick Si_3N_4 AR coating is also shown for reference.

All curves show a clear optimum for 200 nm wide, 175 nm high oblate spheroids in an array with 450 nm pitch. This optimal configuration results in a 35% higher transmission with respect to the bare Si case, corresponding to an overall transmittance of 77%. The Si_3N_4 AR coating yields a 41% enhancement (80% transmittance).

The presence of an optimum in particle width and height is the consequence of a trade-off between different effects. Small particles show strong absorption and small scattering, thus reducing the amount of light transmitted into the substrate. On the other hand, tall particles have a reduced near-field coupling to the substrate, and wide particles have a strongly red-shifted resonance, resulting in a reduced transmittance in the lower-wavelength range due to the Fano effect (see Figure 1). An optimum in the array pitch is also expected, as a smaller pitch also results in an undesired red shift of the plasmonic resonance, due to a stronger coupling between the particles, and a large pitch corresponds to a small surface coverage, reducing the overall light scattering. It is important to note that the overall transmission enhancement is most sensitive to array pitch (Figure 2c). This implies that self-assembly techniques in which pitch is not well controlled are not suitable for the fabrication of these arrays.

Figure 3 shows the enhancement factor, defined as before, for 200 nm wide Ag spheroids with an array pitch of 450 nm, placed on a Si_3N_4 spacer layer over a Si substrate. Data are shown as a function of particle height with a 50 nm thick Si_3N_4 spacer layer (a), and for 125 nm high particles as a function of Si_3N_4 layer thickness (b). Particle width and array pitch were taken equal to the optimal values found in Figure 2. The introduction of the spacer layer made it necessary to reoptimize the particle height, as the dielectric layer affects the near-field coupling to the substrate.

Figure 3a shows an optimal particle height of 125 nm, which is reduced compared to the optimum height without the spacer layer (Figure 2, 175 nm). Figure 3b shows an optimal thickness of 50 nm for the Si_3N_4 spacer layer. For this configuration, a net incoupling enhancement of 49% with respect to the bare Si case is found, a value 8% higher than that for the standard 80 nm Si_3N_4 AR coating. The maximum value for the absolute transmittance is 84%.

The reduction of the optimal particle height is the result of an optimized near-field coupling between the particle and the Si substrate, since the distance between the particle and the substrate has been increased due to the introduction of a spacer layer. An optimum in Si_3N_4 thickness is found as thicker spacer

dx.doi.org/10.1021/nl200321u |*Nano Lett.* 2011, 11, 1760–1765

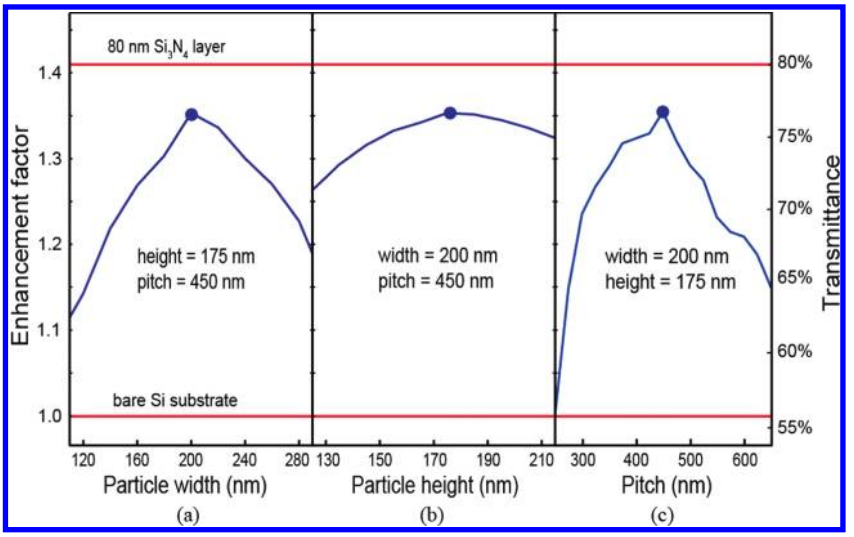

Figure 2. Transmission enhancement for Ag nanoparticle arrays on top of Si, for different geometries, varying particle width (a), height (b), and array pitch (c), integrated over the AM1.5 solar spectrum, relative to a bare Si substrate. The optimal configuration (solid dots) yields 35% better light incoupling with respect to bare Si and an overall integrated transmittance of 77%. The enhancement due to an 80 nm thick Si_3N_4 AR coating is also shown for reference.

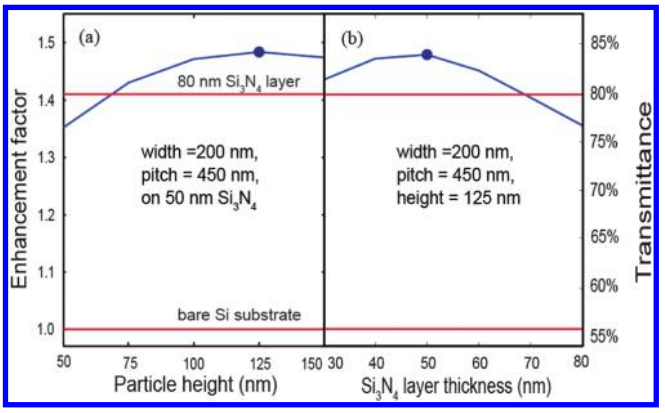

Figure 3. Transmission enhancement for Ag particle arrays on Si with a Si_3N_4 spacer layer, integrated over the AM1.5 solar spectrum, relative to a bare Si substrate. Data are shown for different particle heights with a 50 nm spacer layer (a) and for 125 nm high particles as a function of Si_3N_4 spacer layer thickness (b). The best geometry increases the light incoupling by almost 50% with respect to bare Si, 8% higher than for a standard AR coating on Si.

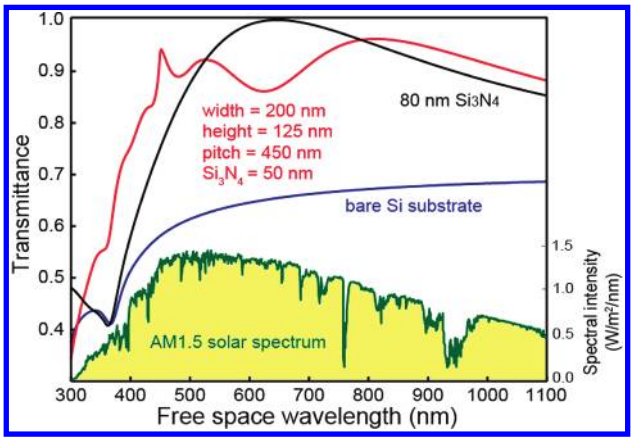

Figure 4. Spectra of transmission into Si for a bare Si substrate (blue), a Si substrate coated with 80 nm Si_3N_4 (black, standard AR coating), and the optimal configuration of Ag nanoparticles on a Si_3N_4 spacer layer (red). The presence of the particle array increases the light coupling in the near-infrared region, above 800 nm. The enhanced transmission in the blue is due to the reduced Si_3N_4 layer thickness compared to the 80 nm layer geometry. The AM1.5 solar spectrum is shown for reference.

layers lead to reduced near-field coupling, while thinner layers cause a red shift of the plasmon resonance, as the near-field couples more strongly to the high-index Si substrate.[23] Moreover, the (thinner) Si_3N_4 layer serves as an AR coating in the blue spectral range.

Figure 4 shows the simulated transmittance spectra for a semi-infinite Si substrate (blue), an 80 nm thick Si_3N_4 coated Si substrate (black) and for the optimal nanoparticle array on top of a 50 nm thick Si_3N_4 layer (red). The AM1.5 solar spectrum is also shown for reference (scale on the right axis). The optimized configuration shows a higher transmittance than the standard AR coating over almost the entire spectrum, with the exception of a narrow band around a wavelength of 600 nm. The transmittance enhancement in the blue can be explained by a blue shift of the AR optimum for a 50 nm Si_3N_4 layer, compared to that of a 80 nm thick layer. The enhancement at longer wavelengths is a result of the strong metal particle scattering into the substrate (see also Figure 1). The combination of the two effects results in a plasmonic AR coating that is optimized for a broad spectral range.

Light Scattering from Particle Arrays: Experiment. The enhanced coupling of light into a substrate due to the plasmonic coatings was studied experimentally by means of reflectance spectroscopy. The samples were 300 μm thick p-type single-side polished monocrystalline Si wafers, with a phosphorus-diffused emitter, coated with a Si_3N_4 layer using plasma-enhanced chemical vapor deposition, on top of which Ag nanoparticle arrays were fabricated on top of the Si_3N_4 layer by means of electron beam lithography (EBL), silver evaporation, and lift-off. A scanning electron microscopy (SEM) image of one of the arrays is shown in the inset in Figure 5. The samples have a

dx.doi.org/10.1021/nl200321u |*Nano Lett.* 2011, 11, 1760–1765

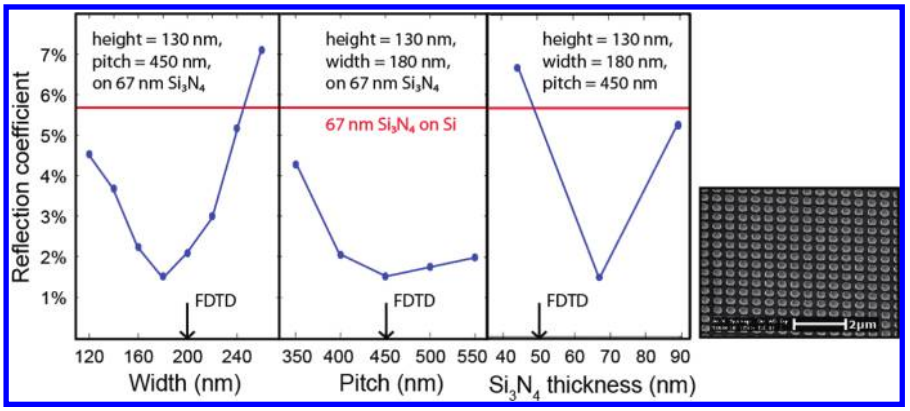

Figure 5. Measured specular reflection coefficient for different particle geometry on a Si substrate, with a Si_3N_4 spacer layer, averaged over the AM1.5 solar spectrum in the 450−900 nm spectral range. The particle width (a), array pitch (b) and Si_3N_4 thickness (c) is varied. The data show a clear minimum, with a reflection coefficient of 1.4%. The red line indicates the reflection coefficient measured on a Si substrate with a 67 nm Si_3N_4 layer (5.7%), for reference. The arrows indicate the configuration for minimum reflectivity found in FDTD (Figure 2). The inset on the right shows a SEM image of a silver nanoparticle array, fabricated by EBL.

uniform Al back contact formed by screen printing. The image clearly shows the dense arrayed Ag particles, with a surface coverage of 20%.

In order to determine experimentally which geometry shows optimal light incoupling, we fabricated different Ag particle arrays in fields of 100 μm by 100 μm, each field with different particle width and array pitch, on samples with different Si_3N_4 thicknesses. The specular reflectance spectrum for each field was measured in an optical microscope, in the wavelength range 450−900 nm. For each field configuration, a reflection coefficient was calculated as the averaged specular reflectance spectrum, weighted by the AM1.5 solar spectrum in the 450−900 nm spectral range. Figure 5 shows the reflection coefficient for varying particle width (a), array pitch (b), and spacer layer thickness (c). The average reflection coefficient for a Si substrate coated with a 67 nm Si_3N_4 layer is also shown for reference (red line, 5.7%).

The trends shown in Figure 5 for the specular reflectance closely match the optima in the simulation results shown in Figure 2, indicated by arrows in Figure 5. An optimal configuration is found for 180 nm wide particles (compared to a 200 nm optimal width from FDTD simulations), with a 450 nm array pitch (same as FDTD). The specular reflection coefficient is reduced from 5.7% to 1.4% by the presence of the particle array. The small deviations between the experimentally found optima and those from the FDTD results are attributed to the differences in particle shape (spheroidal in the simulation, cylinder-like in the experiment) and to the slightly different spectral ranges over which the averages are taken.

In order to investigate the absorption in the Si layer, we have performed measurements of the total reflectivity in an integrating sphere setup. A 2×2 mm^2 array of silver nanoparticles, with the optimal parameters found in Figure 5 was fabricated by using EBL on a sample with a 67 nm thick Si_3N_4 spacer layer. The angle-integrated reflectivity spectra were then measured in the 300−1200 nm spectral range, for an angle of incidence of 8°. Figure 6 shows the total reflectivity spectrum for this sample (blue), and for the same sample without Ag nanoparticles (red).

The reflection spectrum for a Si substrate coated with 67 nm of Si_3N_4 shows the typical trend for an interference AR coating, yielding a minimum in reflection around 600 nm. Adding the

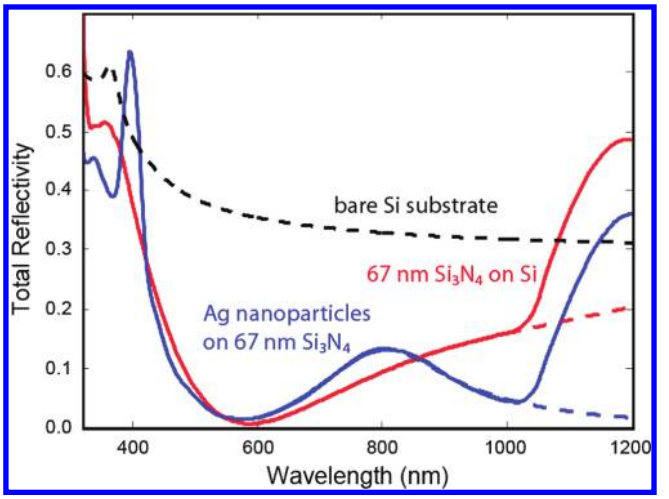

Figure 6. Measured total reflection spectrum from a 300 μm crystalline Si cell coated with 67 nm Si_3N_4 (red) and the same sample with an optimized Ag particle array on top (blue). The particles reduce the reflection for wavelengths above 800 nm, improving the incoupling of light into the Si substrate. The dashed lines are extrapolated data representing the reflection from a semi-infinite substrate. The calculated reflectance of a semi-infinite Si substrate is shown for reference (dashed black line).

particle array yields a broad band reduction in total reflection above 850 nm and, with the exception of the relatively small enhancement in the 600−800 nm range, does not drastically affect the light incoupling for lower wavelengths. Note that the sudden reflection increase above 1050 nm in both curves is due to light that is reflected from the back contact and that is not absorbed in the Si substrate. Indeed, the absorption length of Si at 1050 nm equals 600 μm, i.e., twice the cell thickness. The dashed lines in Figure 6 are extrapolations of the data, representing the reflectivity of a semi-infinite substrate sample, made using a linear fit for the bare substrate (red), and a Lorentian fit for the substrate with particles (blue) on the data set in the 600−1000 nm spectral range.

The total reflection spectrum can be used to calculate the absorption in the solar cell, using the relation: $A = 1 - R - T$,

dx.doi.org/10.1021/nl200321u |*Nano Lett.* 2011, 11, 1760–1765

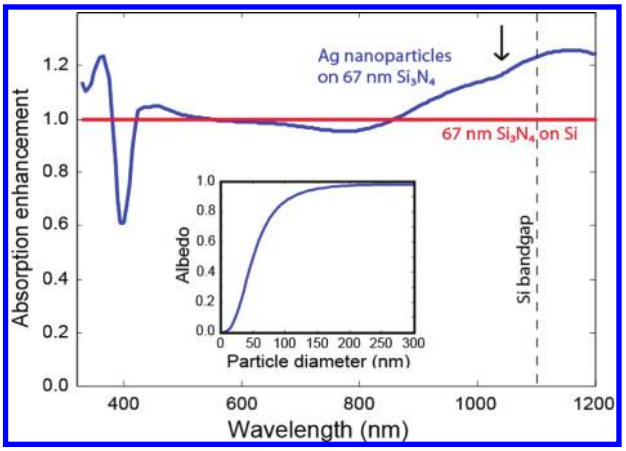

Figure 7. Absorption enhancement due to the presence of a silver nanoparticle array on top of a 67 nm Si_3N_4 layer on a Si substrate. A broad band enhancement is observed in the near-infrared region, for wavelengths above 800 nm. The arrow indicates a small kink in the data that indicates the onset of light trapping. In the inset, the calculated albedo for a silver nanoparticle in air is shown as a function of particle diameter. For 180 nm diameter particles, as used in the experiment, the albedo amounts to 97%, meaning that only 3% of the light is absorbed in the metal.

where A is the absorbance, R the reflectance, and T the transmittance. In this case, T is zero, since the sample has an Al back reflector. Figure 7 shows the calculated absorption spectrum for the sample with the metal nanoparticles on top (blue), normalized to the absorption in the reference sample (67 nm Si_3N_4 on Si, red line). The Si band gap wavelength is also shown in the graph for reference (vertical dashed line).

Figure 7 shows a broad band absorption enhancement above 850 nm, with a peak larger than 120% near the Si band gap wavelength, i.e., in the region where Si is a poor absorber of light. With the exception of a narrow dip around 400 nm, the spectrum below 850 nm is only slightly affected by the presence of the particle array.

Our experimental data clearly demonstrate that metal nanoparticle arrays result in strongly enhanced light coupling and thus enhanced impedance matching into a Si substrate. When compared to a standard AR coating, light coupling is enhanced over a broad spectral range in the near-infrared.

While the major effect observed in this paper is enhanced impedance matching into a Si substrate, a minor light trapping effect is also observed in the total reflectivity measurement in Figure 7. A signature of the light trapping effect can be observed in the small change in the slope of the curve around 1050 nm (see arrow in Figure 7). In the 1050−1200 nm spectral range, i.e., the range where light is not fully absorbed in the 300 μm thick Si substrate, the absorption enhancement in the Si substrate is due to both the AR effect analyzed in this paper and light trapping. On the basis of the data, it is possible to derive a rough estimate of the relative influence of the two different effects on the absorption enhancement. From the extrapolated data in Figure 6 (dashed lines), we can estimate what part of the absorption is purely due to the enhanced AR effect and compare it to the total absorption enhancement measured on the finite-thickness sample (Figure 7). At 1120 nm (Si band gap), we find that the enhancement due to the AR effect amounts to 20%, while the total measured enhancement is found to be 25%. From this we estimate that the remaining 5% of the absorption enhancement is a result of light trapping. The next step is to apply these results on much thinner Si wafers where the effect of light trapping will become apparent at a much broader spectral range and compare it with standard light trapping methods such as surface texturing.

Finally, we point out that the absorption spectrum shown in Figure 7 includes both absorption in the Si substrate and Ohmic dissipation in the metal nanoparticles. The inset in Figure 7 shows the calculated albedo of a silver nanoparticle in air as a function of particle diameter. For particles of 180 nm diameter, as used in the experiment, the albedo amounts to 97%, meaning that only 3% of the light is absorbed in the Ag nanoparticle. For particles on a higher index substrate, the albedo is even higher, as the scattering is enhanced due to the higher density of states in the substrate. It is therefore correct to neglect dissipation in the metal nanoparticles and attribute the absorption measured in Figure 7 solely to the Si substrate.

Conclusions. We have performed a systematic study of light coupling to a Si substrate coated with an array of Ag nanoparticles that show a strong plasmon resonance. We have shown by means of FDTD simulations that a properly chosen array of Ag nanoparticles on a Si_3N_4 spacer layer acts as a better antireflection coating than a standard Si_3N_4 interference coating, over a broad spectral range. The coupling is determined by competing effects of Fano resonances in the scattering, interparticle coupling, and resonance shifts due to variations in the near-field coupling to the substrate and spacer layer. We find that 200 nm wide, 125 nm high spheroidal Ag particles in a square array with 450 nm pitch on top of a 50 nm thick Si_3N_4 layer provide the best impedance matching for a spectral distribution corresponding to the AM1.5 solar spectrum. Using the optimal array configuration, simulations predict a 8% improvement of light incoupling to Si compared to the best standard interference AR coating and an improvement of almost 50% with respect to a bare Si substrate. Our simulation results are confirmed experimentally by reflection and absorption spectroscopy on fabricated Ag nanoparticle arrays. For wavelengths near the Si band gap, where light is poorly absorbed, a small light trapping effect is also observed. The results obtained in this work can be used to design antireflection and light trapping coatings for thin Si solar cells and may have applications for photodetectors and other optical components as well.

AUTHOR INFORMATION

Corresponding Author
*E-mail: spinelli@amolf.nl.

ACKNOWLEDGMENT

This work is part of the research program of the Foundation for Fundamental Research on Matter (FOM) which is financially supported by The Netherlands Organization for Fundamental Research (NWO). It is also part of the Global Climate and Energy Project (GCEP).

REFERENCES

(1) Atwater, H. A.; Polman, A. *Nat. Mater.* **2010**, *9*, 205.
(2) Catchpole, K. R.; Polman, A. *Opt. Express* **2008**, *16*, 21793.
(3) Stuart, H. R.; Hall, D. G. *Appl. Phys. Lett.* **1996**, *69*, 2327.
(4) Stuart, H. R.; Hall, D. G. *Appl. Phys. Lett.* **1998**, *73*, 3815.

(5) Schaadt, D. M.; Feng, B.; Yu, E. T. *Appl. Phys. Lett.* **2005**, *86*, No. 63106.
(6) Derkacs, D.; et al. *Appl. Phys. Lett.* **2006**, *89*, No. 93103.
(7) Derkacs, D.; et al. *Appl. Phys. Lett.* **2008**, *93*, No. 091107.
(8) Pillai, S.; et al. *J. Appl. Phys.* **2007**, *101*, No. 93105.
(9) Nakayama, K.; Tanabe, K.; Atwater, H. *Appl. Phys. Lett.* **2008**, *93*, No. 121904.
(10) Catchpole, K. R.; Polman, A. *Appl. Phys. Lett.* **2008**, *93*, No. 191113.
(11) Beck, F. J.; Polman, A.; Catchpole, K. R. *J. Appl. Phys.* **2009**, *105*, No. 114310.
(12) Mokkapati, S.; et al. *Appl. Phys. Lett.* **2009**, *95*, No. 053115.
(13) Temple, T. L.; et al. *Sol. Energy Mater. Sol. Cells* **1978**, *93*, 2009.
(14) Matheu, P.; et al. *Appl. Phys. Lett.* **2008**, *93*, No. 113108.
(15) Ferry, V.; et al. *Opt. Express* **2010**, *18*, A237.
(16) FDTD solutions (www.lumerical.com)
(17) Palik, E. D. *Handbook of Optical Constants of Solids*; Academic: New York, 1985.
(18) Kippenberg, T. J.; et al. *Phys. Rev. Lett.* **2009**, *103*, No. 027406.
(19) Lim, S. H.; et al. *J. Appl. Phys.* **2007**, *101*, No. 106309.
(20) Mirin, N. A.; Bao, K.; Nordlander, P. *J. Phys. Chem. A* **2009**, *113*, 4028.
(21) Luk'yanchuk, B.; et al. *Nat. Mater.* **2010**, *9*, 707.
(22) Lassiter, J. B.; Sobhani, H.; Fan, J. A.; Kundu, J.; Capasso, F.; Nordlander, P.; Halas, N. J. *Nano Lett.* **2010**, *10*, 3184.
(23) Xu, G.; et al. *Appl. Phys. Lett.* **2003**, *82*, 3811.